A&A 393, 721–726 (2002)
DOI: 10.1051/0004-6361:20021174

Astronomy & Astrophysics

Ion contribution to the astrophysical important 447.15, 587.56 and 667.82 nm He I spectral lines broadening

V. Milosavljević[1,2] and S. Djeniže[1,2,3,⋆]

[1] Faculty of Physics, University of Belgrade, PO Box 368, Belgrade, Serbia, Yugoslavia
[2] Isaac Newton Institute of Chile, Yugoslavia Branch, Belgrade, Yugoslavia
[3] Hungarian Academy of Sciences, Budapest, Hungary

Received 16 May 2002 / Accepted 9 August 2002

Abstract. Characteristics of the astrophysical important Stark broadened 447.15 nm, 587.56 nm and 667.82 nm He I spectral line profiles have been measured at electron densities between 0.3×10^{22} and 8.2×10^{22} m^{-3} and electron temperatures between 8000 and 33 000 K in plasmas created in five various discharge conditions using a linear, low-pressure, pulsed arc as an optically thin plasma source operated in a helium-nitrogen-oxygen gas mixture. On the basis of the observed asymmetry of the line profiles we have obtained their ion broadening parameters (A) caused by influence of the ion microfield on the line broadening mechanism and also the influence of the ion dynamic effect (D) on the line shape. Our A and D parameters represent the first data obtained experimentally by the use of the line profile deconvolution procedure. We have found stronger influence of the ion contribution to these He I line profiles than the semiclassical theoretical approximation provides. This can be important for some astrophysical plasma modeling or diagnostics.

Key words. plasmas – line: profiles – atomic data

1. Introduction

After hydrogen, helium is the most abundant element in the universe. Helium atoms and ions are present in many kinds of cosmic light sources and their radiation is very useful for astrophysical plasma diagnostical purposes (Griem 1974, 1997). In spite of this special role have the 447.15 nm ($2p\ ^3P^0_{2,1}$–$4d\ ^3D_{3,2,1}$ transition), 587.56 nm ($2p\ ^3P^0_{2,1}$–$3d\ ^3D_{3,2,1}$ transition) and 667.82 nm ($2p\ ^1P^0_1$–$3d\ ^1D_2$ transition) neutral helium (He I) spectral lines. Recently, in the work by Benjamin et al. (2002) these have been used to investigate the radiative transfer effects for a spherically symmetric nebula with no systematic velocity gradients. Izotov et al. (2001) use these lines to derive the ^{4}He abundance in the Metal-deficient Blue Compact Dwarf Galaxies Tol 1214-277 and Tol 65[1]. In the work by Harvin et al. (2002) the 667.82 nm line profile has been used to investigate the physical properties of the Massive Compact Binary in the Triple Star System HD 36486 (δ Orionis A). The 587.56 nm spectral line has been used by Labrosse & Gouttebroze (2001) to estimate the formation of the helium spectrum in solar quiescent prominences and, also, by Muglach & Schmidt (2001) to determine the height and dynamics of the quiet solar chromosphere at the limb. Therefore, the use of these He I spectral lines for diagnostic purposes in astrophysics needs the knowledge of their line profile characteristics. In plasmas with electron densities (N) higher than 10^{21} m^{-3}, where the Stark effect begins to play an important role by the He I spectral lines broadening, knowledge of the Stark broadening characteristics is necessary. A significant number of theoretical and experimental studies are devoted to the He I Stark $FWHM$ (full-width at half intensity maximum, W) investigations (Lesage & Fuhr 1999, and references therein). The aim of this work is to present measured Stark broadening parameters of the mentioned He I spectral lines at (8000–33 000) K electron temperatures (T) and at electron densities of $(0.3–8.2)\times10^{22}$ m^{-3}. The T-values used are typical for many cosmic light sources. Using a deconvolution procedure described by Milosavljević & Poparić (2001) we have obtained, for the first time, on the basis of the observed line profile asymmetry, the ion contribution to the line shape from the quasistatic ion (parameter A) and ion dynamic effect (coefficient D) (Griem 1974; Barnard et al. 1974; Bassalo et al. 1982) and, also, the separate electron (W_e) and ion (W_i) contributions to the total Stark width (W_t). As a plasma source we have used a linear, low-pressure, pulsed arc operated in five various discharge conditions. Our measured W_t, W_e, W_i and A values have been compared to all available theoretical and experimental data.

2. Experiment

The modified version of the linear low pressure pulsed arc (Djeniže et al. 1992, 1998, 2002; Milosavljević et al. 2000, 2001) has been used as a plasma source. A pulsed discharge

Send offprint requests to: V. Milosavljević,
e-mail: vladimir@ff.bg.ac.yu
⋆ e-mail: steva@ff.bg.ac.yu

Table 1. Various discharge conditions. C-bank capacity (in μF), U-bank voltage (in kV), H-plasma length (in cm), Φ-tube diameter (in mm), P-filling pressure (in Pa). N (in 10^{22} m^{-3}) and T (in 10^3 K) denote electron density and temperature values, respectively obtained at the 25th μs (index 1) and 120th μs (index 2) after the beginning of the discharge when the profiles were analyzed.

C	U	H	Φ	P	N_1	N_2	T_1	T_2
8	4.5	6.2	5	267	6.1	0.7	33.0	16.0
14	4.2	14.0	25	267	8.2	0.9	31.5	14.5
14	3.4	14.0	25	267	6.7	0.8	30.0	14.0
14	2.6	14.0	25	267	4.4	0.3	28.0	12.5
14	1.5	7.2	5	133	5.0	0.6	18.0	8.0

was driven in a quartz discharge tube at different inner diameters and plasma lengths. Varying the dimensions of the discharge tube offers the possibility of electron temperature variation within a wide range. The working gas was helium – nitrogen – oxygen mixture (90% He + 8% N_2 + 2% O_2). The tube geometry used and the corresponding discharge conditions are presented in Table 1.

Spectroscopic observation of spectral lines was made end-on along the axis of the discharge tube with (1.8–2.0) mm beam diameter.

The line profiles were recorded by a step-by-step technique using a photomultiplier (EMI 9789 QB and EMI 9659B) and a grating spectrograph (Zeiss PGS-2, reciprocal linear dispersion 0.73 nm/mm in the first order) system. The instrumental $FWHM$ of 8 pm was obtained by using narrow spectral lines emitted by the hollow cathode discharge. The spectrograph exit slit (10 μm) with the calibrated photomultipliers was micrometrically traversed along the spectral plane in small wavelength steps (7.3 pm). The averaged photomultiplier signal (five shots in each position) was digitized using an oscilloscope, interfaced to a computer.

The plasma reproducibility was monitored by the He I (501.5 nm, 388.8 nm and 587.6 nm) lines radiation and, also, by the discharge current using the Rogowski coil signal (it was found to be within ±5%). Using the double plasma length method, described in Milosavljević (2001), an absence of self-absorption was found in the case of the investigated line profiles.

The details of the deconvolution procedure used were described by Milosavljević & Poparić (2001) and Milosavljević (2001), and summarized in Sect. 3. Briefly, it concerns a new advanced numerical procedure for the deconvolution of theoretical asymmetric convolution integral of a Gaussian and a plasma broadened spectral line profile $j_{A,R}(\lambda)$ for spectral lines. This method gives complete information on the plasma parameters from a single recorded spectral line. The method determines all broadening (W_t, W_e, W_i, A and D) and plasma parameters (N and T) self-consistently and directly from the shape of spectral lines without any assumptions or prior knowledge. All one needs to know is the instrumental width of the spectrometer. The measured profiles are the result of convolution of the spectral line profiles by Lorentzian and Stark broadening, and by Doppler and instrumental broadening; the last two have Gaussian profiles. Van der Waals and resonance broadenings (Griem 1974) were estimated to be smaller by more than an order of magnitude in comparison to Stark, Doppler and instrumental broadenings. The deconvolution procedure was computed using the least Chi-square function (Milosavljević & Poparić 2001; Milosavljević 2001) (see Sect. 3).

The plasma parameters were determined using standard diagnostic methods. Thus, the electron temperature was determined from the ratios of the relative line intensities of four N III spectral lines (409.74 nm, 410.34 nm, 463.42 nm and 464.06 nm) to the 463.05 nm N II spectral line with an estimated error of ±10% (for index 1 in Table 1) and ±30% (for index 2 in Table 1), assuming the existence of LTE (Griem 1974). All the necessary atomic data were taken from NIST (2002) and Glenzer et al. (1994). The electron density decay was measured using a well-known single wavelength He-Ne laser interferometer technique (with 1.5 mm laser beam diameter) for the 632.8 nm transition with an estimated error of ±9% (for index 1 in Table 1) and ±50% (for index 2 in Table 1). The electron densities and temperatures, obtained at the moment when the line profiles were analyzed, are presented in Table 1.

We monitored the 447.15 nm line profile up to the 120th μs after the beginning of the discharge when the electron density has dropped down to (3.0–9.0)×10^{21} m^{-3} and the electron temperature to (8000–16 000) K. With these plasma parameters the 447.15 nm line can be used as isolated and separated from its 447.0 nm forbidden component (Milosavljević & Djeniže 2001). The asymmetric 447.15 nm line profile, as example, is presented in Fig. 1 with the obtained broadening parameters and its negligible forbidden component.

3. Numerical procedure for deconvolution

The proposed function for various line shapes, Eq. (1) is of the integral form and includes several parameters. Some of these parameters can be determined in separate experiments, but not all of them. Furthermore, it is impossible to find an analytical solution for the integrals and methods of numerical integration to be applied. This procedure, combined with the simultaneous fitting of several free parameters, requires a number of computer-supported mathematical techniques.

$$K(\lambda) = K_o + K_{max} \int_{-\infty}^{\infty} \exp(-t^2) \cdot \times \left[\int_0^{\infty} \frac{H_R(\beta)}{1 + \left(2 \frac{\lambda - \lambda_o - \frac{W_G}{2\sqrt{\ln 2}} \cdot t}{W_e} - \alpha \cdot \beta^2 \right)^2} \cdot d\beta \right] \cdot dt. \quad (1)$$

Here K_o is the baseline (offset) and K_{max} is the maximum of intensity (intensity for $\lambda = \lambda_o$) Milosavljević & Poparić (2001). $H_R(\beta)$ is an electric microfield strength distribution function of normalized field strength $\beta = F/F_o$, where F_o is the Holtsmark field strength. A ($\alpha = A^{4/3}$) is the static ion broadening parameter as a measure of the relative importance of ion and electron broadenings. R is the ratio of the mean distance between the

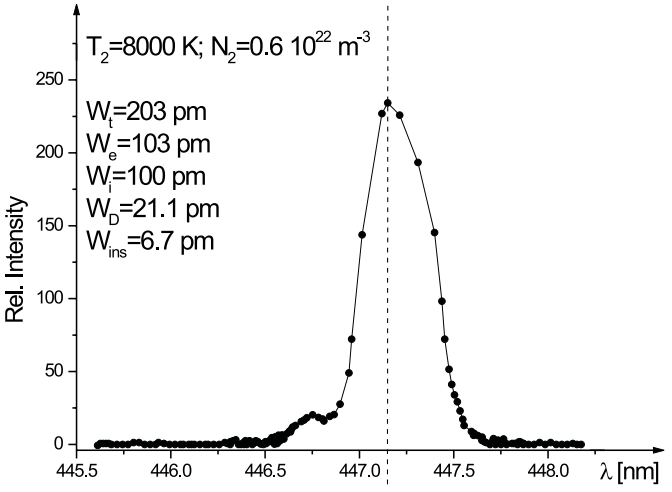

Fig. 1. Recorded profile of the 447.15 nm line at given T and N. W_t, W_e, W_i, W_D, W_{ins}, represent total, electron and ion Stark width, Doppler and instrumental width, respectively.

ions to the Debye radius, i.e. the Debye shielding parameter and W_e is the width ($FWHM$) of the $j_{A,R}$ profile (Griem 1974).

For the purpose of the deconvolution iteration process we need to know the value of K function (1) as a function of λ for every group of parameters (K_{max}, λ_o, W_e, W_G, R, A). The function $K(\lambda)$ is in integral form and we have to solve a triple integral in each step of the iteration process of varying the above group of parameters. The first integral in the K function is the microfield strength distribution function, $H_R(\beta)$, the second one is the $j_{A,R}(\lambda)$ function, and the third is the convolution integral of a Gaussian with a plasma broadened spectral line profile $j_{A,R}(\lambda)$ (denoted by $K(\lambda)$ in Eq. (1)). None of these integrals has an analytic solution and they must be solved using numerical integration (Milosavljević & Poparić 2001; Milosavljević 2001).

After numerical integration the fitting procedure itself can be started. For Eq. (1), the fitting procedure will give the values for W_G, W_e, λ_o, R, A and K_{max}.

We use the standard manner of defining the best fit: the sum of the squares of the deviations (χ^2) of the theoretical function from the experimental points is at its minimum. The necessary condition for the minimum of $\Sigma\chi^2$ is that the partial derivatives of the function are equal to zero. Therefore, for the K profile we have a system of six nonlinear homogeneous equations with six parameters. The numerical solutions of these systems are found using Newton's method of successive approximations (Milosavljević & Poparić 2001; Milosavljević 2001).

Newton's method requires successive solving of the inverse Jacobi matrices of the system of equations for each step, which are subject to rounding errors. Moreover, the numerical partial derivatives in Jacobi matrix itself are sources of rounding errors. These rounding errors destabilize the convergence of the system, although all mathematical conditions are fulfilled. The algorithm may be stabilized by reducing the iteration procedure to independent parameters only (Milosavljević & Poparić 2001; Milosavljević 2001).

This sophisticated deconvolution method, which allows the direct determining of all six parameters by fitting theoretical K-profile (1), to experimental data, requires a sufficient number of experimental points per line, and small statistical errors. The method requires a minimum of twenty experimental points per line (the border of line is $(-3/2\cdot W_e+\lambda_o < \lambda < +3/2\cdot W_e+\lambda_o)$, where W_e is the $FWHM$), and the maximal statistical indeterminacy in intensity is 5% at every experimental point.

4. Results and discussion

The plasma-broadening parameters (W_t, W_e, W_i, A, D) of the recorded line profiles at measured N and T values obtained by our deconvolution procedure are presented in Table 2 together with the results of other authors. Various theoretical (G, BCW, DSB) predictions of the W_e, W_i, and A are also given. For the normalization of the A^G and A^{BCW} values to our electron density the $N^{1/4}$ numerical factor (Griem 1974) was used.

In order to make the comparison between measured (W_t^{exp}) and calculated (W_t^{th}) total (electron + ion) width values easier, the dependence of the ratio W_t^{exp}/W_t^{th} on the electron temperature is presented graphically in Figs. 2–4 for the three researched lines.

The W_t^G (Griem 1974) and W_t^{BCW} (Bassalo et al. 1982) values are calculated using Eq. (226) from Griem (1974) with the W_e and A values predicted by the G (Griem 1974) and BCW (Bassalo et al. 1982) theoretical approaches, respectively. The W_t^{exp}/W_t^{th} ratios related to the Dimitrijević & Sahal–Bréchot (1990) data have been calculated only for our experimental values. Namely, for the W_i^{DSB} calculations it is necessary to know the helium ion concentration connected to the plasma composition. We have performed this for our discharge conditions only.

It turns out that our W_e^{exp} and W_i^{exp} are the first separate experimental electron and ion Stark width results obtained by using our deconvolution procedure (Milosavljević & Poparić 2001). Our W_e^{exp} results are smaller than the G approximation for all the three investigated lines. The greatest disagreement was found for the 447.15 nm line. It is about 53%. The other two approximations (BCW and DSB), in the case of the 667.82 nm and 447.15 nm lines, provide smaller W_e values than the G approximation, but they are also higher than ours. For the 587.56 nm line the W_e^{exp}, W_e^{BCW} and W_e^{DSB} values show a reasonable mutual agreement (within ±12% experimental accuracy). It is pointed out that the W_e values calculated by Freudenstein & Cooper (1978) and Dimitrijević & Konjević (1986), for the 667.82 nm line, exceed all other W_e data presented in Table 2.

Inspecting Figs. 2–4 one can conclude that the Griem (1974) W_t values lie above all experimental and theoretical data except the results from experiments reported by Purić et al. (1970), Mijatović et al. (1995) and Kelleher (1981). This is clear in the case of the 667.82 nm line at higher electron temperatures (see Fig. 3). Theoretical W_t values presented by Bassalo et al. (1982) lie about 10%–30% below Griem's values. The W_t values (W_e + W_i) presented by Dimitrijević & Sahal–Bréchot (1990) agree with ours (W_t^{exp}) to within

Table 2. Line Broadening characteristics. Measured: total Stark $FWHM$ (W_t^{exp} in pm within ±12% accuracy), electron Stark width (W_e^{exp} in pm within ±12% accuracy), ion Stark width (W_i^{exp} in pm within ±12% accuracy), static ion broadening parameter (A^{exp}, dimensionless within ±15% accuracy) and ion dynamic coefficient (D^{exp}, dimensionless within ±20% accuracy) at a given electron temperature (T in 10^3 K) and electron density (N in 10^{22} m^{-3}). Ref presents the values given in this work (Tw) and those used from other authors: K, Kelleher (1981); B, Berg et al. (1962); KK, Kobilarov et al. (1989); RS, Roder & Stampa (1964); PL, Purić et al. (1970); BG, Büscher et al. (1995); P, Pérez et al. (1991); M, Mijatović et al. (1995); Ga, Gauthier et al. (1981); VK, Vujičić & Kobilarov (1988). The index G, BCW and DSB denote theoretical data taken from Griem (1974), Bassalo et al. (1982) and Dimitrijević & Sahal–Bréchot (1990), respectively at a given T and N.

T	N	W_t^{exp}	W_e^{exp}	W_i^{exp}	A^{exp}	D^{exp}	Ref.	W_e^G	W_e^{BCW}	W_e^{DSB}	W_i^{DSB}	A^G	A^{BCW}
							587.56 nm						
33.0	6.1	210	172	38	0.163	1.46	Tw	215	156	183	42	0.093	0.118
31.5	8.2	268	218	50	0.176	1.40	Tw	289	213	246	55	0.100	0.127
30.0	6.7	218	179	39	0.167	1.46	Tw	237	175	201	45	0.095	0.120
28.0	4.4	151	126	25	0.150	1.57	Tw	155	117	132	29	0.086	0.108
18.0	5.0	150	126	24	0.156	1.60	Tw	176	134	150	31	0.088	0.108
20.9	1.03	39					K						
45.0	15.9	550					B						
31.0	5.4	200					KK						
16.5	1.7				0.05*		RS						
3.70	2.25	91					PL						
52.0	10.2	3160					BG						
							667.82 nm						
33.0	6.1	481	298	183	0.459	1.18	Tw	397	345	358	170	0.282	0.309
31.5	8.2	628	370	258	0.498	1.12	Tw	533	467	502	226	0.300	0.328
30.0	6.7	512	315	197	0.474	1.17	Tw	439	389	402	181	0.282	0.306
28.0	4.4	337	216	121	0.420	1.27	Tw	290	257	266	117	0.252	0.265
18.0	5.0	361	240	121	0.413	1.26	Tw	358	323	323	124	0.249	0.271
20.9	1.03	98					K						
30.1	3.2	231					P						
19.3	0.25	22					M						
20.0	10.0	960					Ga						
26.0	7.1	620					VK						
							447.15 nm						
16.0	0.7	237	106	131	0.917	1.0	Tw	162	150	140	113	0.636	0.668
14.5	0.9	316	145	171	0.911	1.0	Tw	212	200	185	142	0.668	0.704
14.0	0.8	258	120	138	0.883	1.0	Tw	190	180	165	125	0.642	0.675
12.5	0.3	101	48	53	0.806	1.03	Tw	73	69	63	45	0.491	0.517
8.0	0.6	203	103	100	0.825	1.0	Tw	155	147	134	82	0.554	0.574
20.9	1.03	109					K						
20.0	13	4500					B						

3%–18% with the best agreement for the 447.15 nm line (see Fig. 4).

We have found a clear contribution of the ion influence to the line broadening due to the quasistatic ion effect expressed with the ion broadening parameter (A). Our A^{exp} values are the first data obtained directly by the use of the line deconvolution procedure. They are higher than what the G and BCW approaches yield by about: 75% and 38% (for the 587.56 nm line), 40% and 34% (for the 667.82 nm line), 31% and 28% (for the 447.15 nm line), respectively. Furthermore, we have found that the ion dynamic effect, expressed as the D coefficient, multiplies the quasistatic ion contribution by about 1.5 for the 587.56 nm line and 1.2 for the 667.82 nm line. For the 447.15 nm line the ion dynamic effect is negligible ($D = 1$). It should be pointed out that we have found good agreement between our W_i^{exp}/W_t^{exp} and theoretical W_i^{DSB}/W_t^{DSB} (Dimitrijević & Sahal–Bréchot 1990) ratio values. These are: 18.5% (18.0%), 37.5% (30.5%) and 53% (44%) for the 587.56 nm, 667.82 nm and 447.15 nm lines, respectively. As can be seen, this agreement is within the estimated experimental accuracies (±12%) of the W_i^{exp} and W_t^{exp} values. One can conclude that the ion contribution to the total line width increases with the upper-level energy of the transition and plays a more important role than what the G and BCW approximations provide.

It turns out that the single A^{exp} value, obtained by Roder & Stampa (1964), presented with an asterisk in Table 2, represents the 587.56 nm line asymmetry factor obtained at the line half intensity maximum. This is about 2.4 times smaller than our A^{exp} value.

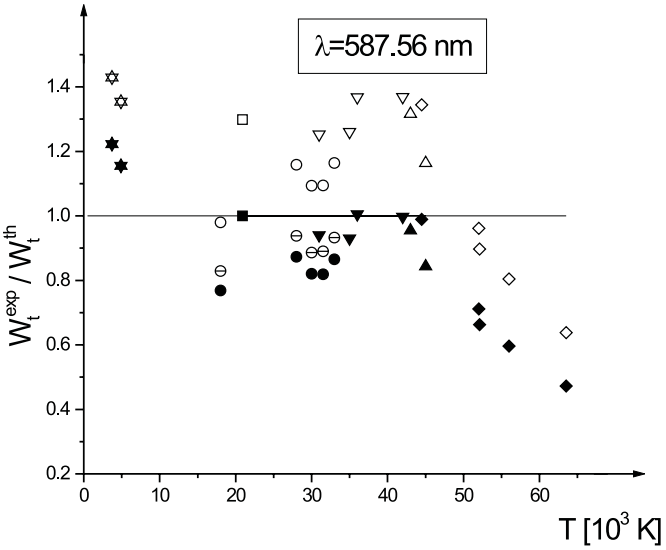

Fig. 2. Ratios of the experimental total Stark $FWHM$ (W_t^{exp}) to the various theoretical (W_t^{th}) predictions vs. electron temperature for λ = 587.56 nm. ◯, ⋄, ∇, △, □ and ✡ represent our experimental data and those from Büscher et al. (1995), Kobilarov et al. (1989), Berg et al. (1962), Kelleher (1981), and Purić et al. (1970), respectively. Filled, empty and half divided symbols represent the ratios related to the theories taken from Griem (1974), Bassalo et al. (1982) and Dimitrijević & Sahal–Bréchot (1990), respectively.

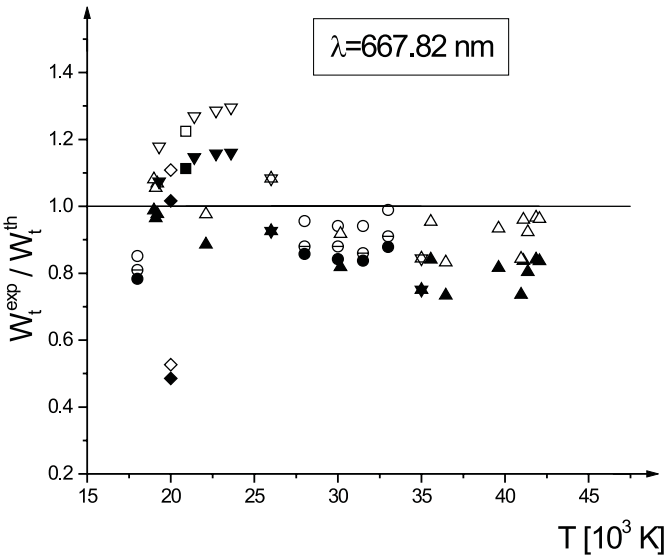

Fig. 3. Ratios of the experimental total Stark $FWHM$ (W_t^{exp}) to the various theoretical (W_t^{th}) predictions vs. electron temperature for λ = 667.82 nm. ◯, ⋄, ∇, △, □ and ✡ represent our experimental data and those from Gauthier et al. (1981), Mijatović et al. (1995), Pérez et al. (1991), Kelleher (1981), and Vujičić & Kobilarov (1988), respectively. Filled, empty and half divided symbols represent the ratios related to the theories taken from Griem (1974), Bassalo et al. (1982) and Dimitrijević & Sahal–Bréchot (1990), respectively.

5. Conclusion

Using a line deconvolution procedure (Milosavljević & Poparić 2001; Milosavljević 2001) we obtained, on the basis of precisely recorded He I spectral line profiles, their Stark broadening parameters: W_t, W_e, W_i, A and D. We found that the ion contribution to the line profiles plays a more important role than the semiclassical approximation provides, which must be taken into account in the use of these He I lines for plasma diagnostical purposes according to the estimations made by the semiclassical perturbation formalism (Dimitrijević & Sahal–Bréchot 1990).

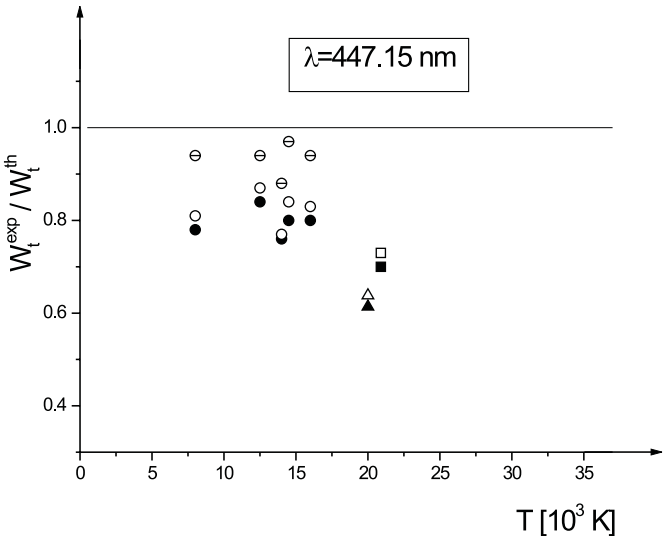

Fig. 4. Ratios of the experimental total Stark $FWHM$ (W_t^{exp}) to the various theoretical (W_t^{th}) predictions vs. electron temperature for λ = 447.15 nm. ◯, △ and □ represent our experimental data and those from Berg et al. (1962) and Kelleher (1981), respectively. Filled, empty and half divided symbols represent the ratios related to the theories taken from Griem (1974), Bassalo et al. (1982) and Dimitrijević & Sahal–Bréchot (1990), respectively.

Acknowledgements. This work is a part of the project "Determination of the atomic parameters on the basis of the spectral line profiles" supported by the Ministry of Science, Technologies and Development of the Republic of Serbia. S. Djeniže is grateful to the Foundation "Arany János Közalapitvány" Budapest, Hungary.

References

Barnard, A. J., Cooper, J., & Smith, E. W. 1974, J. Quant. Spec. Radiat. Transf., 14, 1025
Bassalo, J. M., Cattani, M., & Walder, V. S. 1982, J. Quant. Spec. Radiat. Transf., 28, 75
Benjamin, R. A, Skillman, E. D., & Smits, D. S. 2002, ApJ, 569, 288
Berg, H. F., Ali, A. W., Lincke, R., & Griem, H. R. 1962, Phys. Rev., 125, 199
Büscher, S., Glenzer, S., Wrubel, Th., & Kunze, H.-J. 1995, J. Quant. Spec. Radiat. Transf., 54, 73
Dimitrijević, M. S., & Konjević, N. 1986, A&A, 163, 297
Dimitrijević, M. S., & Sahal−Bréchot, S. 1984, J. Quant. Spec. Radiat. Transf., 31, 301
Dimitrijević, M. S., & Sahal−Bréchot, S. 1990, A&AS, 82, 519
Djeniže, S., Srećković, A., & Labat, J. 1992, A&A, 253, 632
Djeniže, S., Milosavljević, V., & Srećković, A. 1998, J. Quant. Spec. Radiat. Transf., 59, 71
Djeniže, S., Milosavljević, V., & Dimitrijević, M. S. 2002, A&A, 382, 359
Freudenstein, S. A., & Cooper, J. 1978, ApJ, 224, 1079

Gauthier, J. C., Geindre, J. P., Goldbach, C., et al. 1981, J. Phys. B, 14, 2099
Glenzer, S., Kunze, H. J., Musielok, J., Kim, Y., & Wiese, W. 1994, Phys. Rev. A, 49, 221
Griem, H. R. 1974, Spectral Line Broadening by Plasmas (New York: Academic Press)
Griem, H. R. 1997, Principles of Plasma Spectroscopy (Cambridge: University Press)
Harvin, J. A., Gies, D. R., Bagnuolo, W. G. Jr., Penny, L. R., & Thaller, M. L. 2002, ApJ, 565, 1216
Izotov, Y. I., Chaffee, F. H., & Green, R. F. 2001, ApJ, 562, 727
Kelleher, D. E. 1981, J. Quant. Spec. Radiat. Transf., 25, 191
Kobilarov, R., Konjević, N., & Popović, M. V. 1989, Phys. Rev. A, 40, 3871
Labrosse, N., & Gouttebroze, P. 2001, A&A, 380, 323
Lesage, A., & Fuhr, J. R. 1999, Bibliography on Atomic Line Shapes and Shifts, April 1992 through June 1999 (Observatoire de Paris)
Mijatović, Z., Konjević, N., Ivković, M., & Kobilarov, R. 1995, Phys. Rev. E, 51, 4891
Milosavljević, V., Djeniže, S., Dimitrijević, M. S., & Popović, L. Č. 2000, Phys. Rev. E, 62, 4137
Milosavljević, V., & Poparić, G. 2001, Phys. Rev. E, E63, 036404
Milosavljević, V. 2001, Ph.D. Thesis, University of Belgrade, Faculty of Physics, Belgrade (unpublished)
Milosavljević, V., Dimitrijević, M. S., & Djeniže, S. 2001, ApJS, 135, 115
Milosavljević, V., & Djeniže, S. 2001, Eur. Phys. J. D, 15, 99
Muglach, K., & Schmidt, W. 2001, A&A, 379, 592
NIST 2002 - Atomic Spectra Data Base Lines - `http://physics.nist.gov`
Pérez, C., de la Rosa, I., de Frutos, A. M., & Mar, S. 1991, Phys. Rev. A, 44, 6785
Purić, J., Labat, J., Ćirković, Lj., & Konjević, N. 1970, Fizika 2, 67
Roder, O., & Stampa, A. 1964, Z. Phys., 178, 348
Vujičić, B. T., & Kobilarov, R. 1988, 9th Int. Conf. Spect. Line Shapes, Contributed papers (Nicholos Copernicos University press, Torun Poland), A18